Juan SU, Kai-Xuan HE, Deng-Zhu GUO[*], Ying-Jie XING, Geng-Min ZHANG

Key Laboratory for Physics and Chemistry of Nanodevices, Department of Electronics, Peking University, Beijing 100871, China

A vacuum sensor of large measurement scale based on rubbing-processed carbon nanotube films

Abstract. A miniature vacuum sensor with the widest vacuum measurement scale from 5×10^{-6} to 1×10^{5} Pa by using carbon nanotube (CNT) films as the sensing material is presented. The CNT-films were mechanically rubbed onto quartz-glass substrates, with two electrodes evaporated at the two ends. It is found that the resistance of the CNT-films responses sensitively to the change of vacuum pressure. The mechanism of the sensors relates to the adsorption of water molecules which influences the electron transfer in CNTs and increases the CNT-junction resistivity.

Streszczenie: Zaproponowano miniaturowy czujnik próżniowy z szerokim zakresem pomiaru, od $5x10^{-6}$ do $1x10^{5}Pa$, wykorzystujący, jako materiału czułego, błony z nanorurek węglowych (CNT). Błony przetarte są mechanicznie na podłożach ze szkła kwarcowego, na końcach których napylono dwie elektrody. Stwierdzono, że oporność CNT silnie zależy od ciśnienia próżni. Za mechanizm wrażliwości odpowiada adsorpcja cząsteczek wody, co wpływa na przepływ elektronów w CNT i powoduje wzrost oporności złącza CNT. Czujnik próżniowy o szerokim zakresie pomiarów, oparty o przetarte błony z nanorurek węglowych

Keywords: Carbon Nanotube Films, Vacuum Pressure, Water Adsorption.
Słowa kluczowe: Błony z nanorurek węglowych, Ciśnienie próżni, Adsorbcja wody

Introduction

The total pressure measurement in vacuum technology is very important with wide applications. Usually, the combinations of gauges working under different principles are adopted for the measurement from ambient pressure to high vacuum. For example, Pirani gauges are suitable for the pressure range of $10^{5} - 10^{-1}$ Pa, and ionization gauges with thermionic cathodes adapt to the pressure range from 10^{2} Pa to ultrahigh vacuum. Although the combinations of these gauges are extensively applied in industries and laboratories, they are innately difficult to be incorporated in the quickly developed small vacuum systems, due to their big size, high power consumption, X-ray and visible light radiation, and remarkable outgassing. For these reasons, great efforts have been made to optimize the vacuum sensing structures by employing different technologies, such as microelectromechanical systems (MEMS) [1] and opto-electro-mechanical systems [2,3], and nanomaterial-based designs [4,5]. Since carbon nanotubes (CNTs) have attracted interests in sensor applications for their outstanding physical and chemical properties [6-8], some CNT-based field emission ionization gauges have been carried out [9-11]. However, the degradation of field emission tips at low vacuum restrains their real application.

Recently, a novel concept of CNT-based vacuum sensors based on the electrical conduction detect have been proposed. Kawano et al fabricated a vacuum sensor with pressure range of 1×10^{2} Pa ~ 1×10^{5} Pa by suspending a single multi-walled carbon nanotube (MWCNT) and measure its resistance [12]. Kaul et al suspended a single single-walled carbon nanotube (SWCNT) between two electrodes to form a vacuum sensor with a dynamic range from 1×10^{-4} Pa to 1×10^{5} Pa [13]. Choi et al realized a continuous measurement from 3×10^{-3} Pa to 1×10^{5} Pa by using batch-processed CNTs walls [14]. Although these CNT-based sensors have small size, high sensitivity, and short response time, their manufacturing processes are complicated and expensive, hindering their mass-production. Thus, simpler, cheaper, and more reliable manufacturing methods are expected for the practical use of CNT-based vacuum devices.

In this work, we present a miniature vacuum sensor with the widest vacuum measurement scale from 5×10^{-6} Pa to 1×10^{5} Pa by using carbon nanotube (CNT) films as the sensing material. The sensing mechanism relates to the adsorption of water molecules in the vacuum which influences the CNT-films' resistance.

Experimental

The structure and measuring setup of the CNT-based vacuum sensor is schematically shown in figure 1. The CNTs materials, mainly containing SWCNTs (> 90wt. %), were purchased from Beijing Nachen S&T Ltd. To shorten and disperse the raw CNTs, the CNT-powders were stirred and refluxed in the mixture of concentrated HNO_3 (65%) and H_2SO_4 (98%). Then, the resultant CNTs were rinsed and dried for the further use.

The CNT-films were fabricated by mechanically rubbing the CNTs onto the quartz-glass substrates. The quartz-glass substrates were roughened by 1000 mesh white fused alumina powders on one side, and two through holes were drilled besides the two short sides of the substrates to connect the sensor into the measuring loop. Both the raw and acid-treated CNTs were rubbed onto the roughened surfaces of the substrates respectively. Such CNT-film-making method has advantages of simplicity, low cost, and low process temperature compared with traditional ways [15,16]. Meanwhile, it's also more convenient to dope other materials. Two aluminium electrodes were thermally evaporated onto the two ends of the CNT-film, leaving a part of the CNT-film as the sensing area. The electrodes were connected with the wires through screws matching with the holes.

The performance of the sensors was carried out in a vacuum chamber with an adjustable pressure ranging from 1×10^{-7} Pa to 1×10^{5} Pa, which was detected by a traditional Pirani gauge and an ionization gauge. A leak valve was used to control the pressure in the chamber and inject different gases as well. An adjustable DC voltage source (0~30V) and a digital multimeter (Tektronix DMM4050) were used to drive and detect the sensor. The temperature of the sensing area was detected by a Pt100.
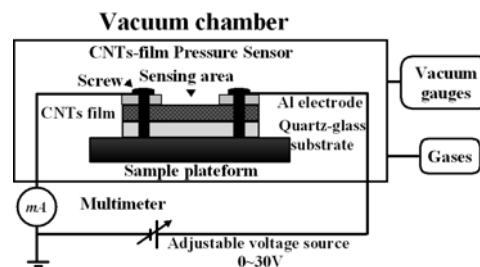

Fig. 1. Schematic of the CNT-film based vacuum sensor and the measuring setup.
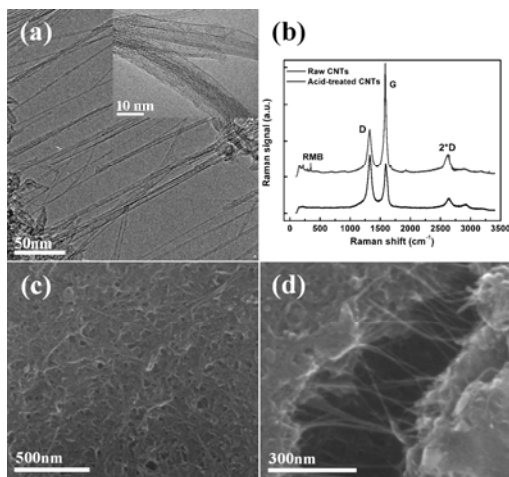
Fig. 2. (a) TEM image of the acid-treated CNTs. The inset is TEM image of the raw CNTs. (b) The Raman spectra from the raw CNT-films (bottom black) and the acid-treated CNT-films (upper red). (c) and (d) SEM images of the CNT-film on quartz-glass substrate on the scale of 500 nm and 300 nm respectively.

Results and discussions

The morphologies of CNTs and the rubbed CNT-films were characterized by using transmission electron microscopy (TEM) and scanning electronic microscopy (SEM). Figure 2(a) and its inset show the TEM images of acid-treated CNTs and raw CNTs. Most of the raw-CNTs bundles are dispersed after the acid treatment, leaving only a few of CNTs still exist in the bundles. To get structural information, Raman spectra from the raw CNT-film and the acid-treated CNT-film are shown in Figure 2(b). In the bottom spectrum from the raw CNT-film, there are two strong peaks around 1593 cm^{-1} and 1333 cm^{-1} whose nomenclatures are G and D. The G line is ascribed to the tangential modes of the graphite-like carbon structure (sp2 hybridization), while the D line is attributed to the defects in graphitic layers, including the curvature of CNT walls and the existence of carbonaceous particles (sp3 hybridization) [17]. In the upper spectrum, in addition to the typical G and D lines of CNTs, two small peaks around 347 cm^{-1} and 227 cm^{-1} appear after the acid treatment, which could be attributes to the radial breathing mode (RBM) of SWCNTs [18]. Meanwhile, the intensity ratio of the D-line to G-line, usually related with the amount of disorders, is 0.68 for the acid-treated CNTs, which is much lower than that of the raw CNTs (~1.2). It is suggested that the CNT-films obtain high crystalline qualities after the acids' surface modification.

The network of CNT-bundles can be observed in the SEM image of the CNT-film on the rough quartz-glass substrate (Fig. 2(c)). After polishing treatment, nearly-uniformly distributed pinholes can be formed in the quartz-glass surfaces, increasing substrates' adhesion to CNTs. CNTs bundles can also be dispersed by the rubbing (Fig. 2(d)), increasing the gas-adsorbing areas of the CNT-films.

The curves of current versus pressure for the sensors based on the raw CNT-films and the acid-treated CNT-films at room temperature are shown in Figure 3(a). Under a constant voltage, the current of the sensor decreased quasi-linearly as the pressure exponentially increased for both sensors, meaning the reduction of the CNT-films' conductance. The continuous pressure response from low-vacuum to high-vacuum for the raw CNT-films (5×10^{-6} Pa~1×10^5 Pa) and the acid-treated CNT-films (5×10^{-4} Pa~1×10^5 Pa) are wider compared to the previous reports [12-14]. In addition, the resistance change of the acid-treated CNT-film (hundreds of ohms) is much larger than that of the raw CNT-film (dozens of ohms) in the same

pressure range, which might be attributed to the improvement of CNTs' crystalline quality after the acid treatment.

In order to detect the sensitivity of the sensor, the resistance change of the acid-treated CNT-film was recorded every 10s while the pressure was changed between two levels. As shown in Figure 3(b), the response delays slightly when a continuous change in air pressure is done within 1600s, indicating the possibility of future application by the further improvement.
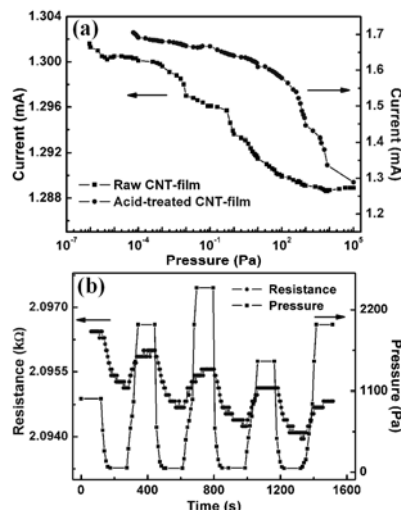

Fig. 3. (a) The current versus the pressure curves of raw CNT-film (square black) and acid-treated CNT-film (circle blue) based sensors in air at the room temperature. (b) Continuous resistance change versus time of an acid-treated CNT-film with a pressure control under the air environment.

In the previous report [12-14], researchers consider that the negative temperature coefficient of CNTs' resistance and the temperature dependent tunneling rate through the CNT/electrodes junction enable the vacuum pressure sensing because the heat transfer rate between CNT and the surrounding gas molecules differs depending on pressure, which is called electro-thermal effect. However, the temperature is not the only influencing factor for the resistance change in our case. In Figure 4(a), when the pressure changes, the temperature change is only 0.4 ℃, while the CNT-film's resistance decreases 11.7 Ω, which is much larger compared with the detected negative temperature coefficient of resistance of this film (about -2.29 Ω/℃), as shown in the inset. It indicates that the resistance change caused by temperature is negligible.

To find the pressure sensing mechanism of the sensor, the pressure responses of the sensor in N_2, Ar, He, and O_2 are also detected, which are similar to that in air (Fig. 4(b)). However, the response strength in air is the strongest, and the linearity is also better than that in other gases. Since water is an important composition of air except O_2, N_2, and inert gases, we inferred that the water adsorption is probably responsible for this change. It can be further demonstrated by the data shown in Figure 4(c), where the decrease of the CNT-film's conductance is about 5 % when the relative humidity of the air increases from 43 % to 97 %.

In vacuum systems, water is one of the main residual gases because the adsorbed water molecules on surfaces could not be easily removed except special outgassing processes. Here we attribute the above conductance response to the adsorption and desorption of the residual water molecules in the vacuum. The influence of water on the conductance of CNT-film can be considered from two aspects. First, the adsorption of water molecules could alter

the carriers' density in the CNTs, causing their conductance change [19,20]. As a polar molecule, water interacts with CNTs through the orientation force that the physisorption is equivalent to the dipole adsorption. Therefore, the amount change of water can induce the change of the surface electrical dipole moment as well as the energy level of the CNTs, and cause the transfer of electrons. Compared with the other nonpolar molecules in air, like N_2, O_2, the influence to the energy level of the CNTs from water is stronger. Second, by introducing the Neugebauer-Webb model [21], the adsorption of water molecules could also increase the resistance of the CNT-junctions because the water surface tension will reduce the Van der Waals' force in CNTs to increase the distances between the CNTs, which may raise the tunneling potential barrier so as to increase the junction resistance. Thus, the water adsorption plays a key role in the resistivity change of CNT-films.
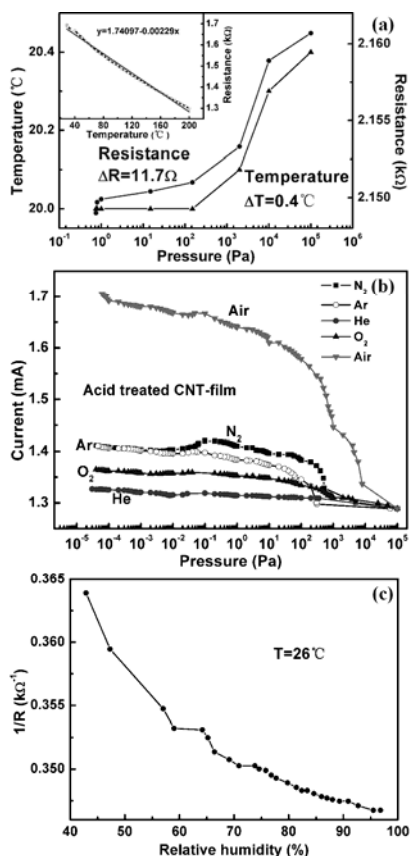

Fig. 4. (a) The temperature change in chamber over pressure (black triangle), and the corresponding resistance change (blue circle). The inset shows the temperature dependence of the CNT-film resistance. (b) The current versus the pressure curve of the sensor based on the acid-treated CNT-film in N_2, Ar, O_2, He, and air. (c) The resistance versus relative humidity curve of the CNT-film at room temperature.

To find the relationship between the conductance of the sensors and the vacuum pressure, the conductivity of the CNT-films is calculated based on the function of $\sigma=(n_0-\Delta n)e\mu$, were n_0 is the carriers density without water on the surface and Δn is the depleted carrier concentration after adsorption of water molecules. By considering adsorption /desorption rates of water molecules and the amount of water in the environment, the conductivity at a low humidity condition is

(1)
$$\sigma = \frac{1}{\rho} = \sigma_0 - aNM_0bP_we\mu,$$

where ρ is the resistivity of the CNT-films, a is the number of electron transported to CNTs after adsorbing one water molecule, M_0 is the mole number of the adsorbed water under saturation, P_w is the water vapor pressure, N is the Avogadro constant, and b is a constant. The conductivity is negatively proportional to the water pressure P_w which is proportional to the relative humidity in the air, agreeing with the conductance changing trend in Figure 4(c). In vacuum, the amount of adsorbed water on CNTs is proportional to the water molecule density, which could be represented by water partial pressure. Therefore, the measured conductance also has a good response to the vacuum pressure.

Moreover, the larger resistance change in the acid-treated CNT-film compared to that of the raw CNT-film (Figure 3(a)) may be attributed to the introduction of more functional groups to the CNTs after the acid treatment [22,23]. The increased dangling bands will enhance the water adsorbing ability to the CNTs, so that the acid-treated CNT-films are more sensitive to vacuum pressure than the raw ones.

Conclusion

In this work, a vacuum sensor was fabricated by rubbing CNTs onto quartz-glass substrates mechanically to form the CNT-films and evaporating Al electrodes on the surface of as-prepared CNT-films, and shows wide vacuum measurement scale from rough-vacuum to high-vacuum. The pressure sensing mechanism of the CNT-films is attributed to the water molecules adsorption, which causes the change of CNT-film's resistance. The present work sheds light on the promising of a new type miniature vacuum sensor with wide measurement range, high response sensitivity, and high manufacturing yield through further CNT surface modification, size reduction, and external circuit improvement.

Acknowledgements

REFERENCES
[1] He F., Huang Q. A., Qin M., A silicon directly bonded capacitive absolute pressure sensor, Sens. Actuators A 135 (2007) 507-514.
[2] Pelletier N., Beche B., Tahani N., Zyss J., Camberlein L., Gaviot E., SU-8 waveguiding interferometric micro-sensor for gage pressure measurement, Sens. Actuators A 135 (2007) 179-184.
[3] Porte H., Gorel V., Kiryenko S., Goedgebuer J. P., Daniau W., Blind P., Imbalanced Mach-Zehnder interferometer integrated in micromachined silicon substrate for pressure sensor, J. Lightwave Technol. 17 (1999) 229-233.
[4] Wei T. Y, Yeh P. H., Lu S. Y, Wang Z. L., Gingatic enhancement in sensitivity using Schottky contacted nanowire nanosensor, J. Am. Chem. Soc. 131 (2009) 17690-5.
[5] Wu L. M., Song F. F., Fang X. X., Guo Z. X., Liang S., A practical vacuum sensor based on a ZnO nanowire array, Nanotechnology 21 (2010) 475502.
[6] Iijima S., Ichihashi T., Ando Y., Pentagons, heptagons and negative curvature in graphite microtubule growth, Nature 356 (1992) 776-778.
[7] Baughman R. H., Zakhidov A. A., de Heer W. A., Carbon nanotubes-the route toward applications, Science 297 (2002) 787-792.
[8] Dresselhaus M. S., Dresselhaus G., Avouris Ph., Topics in Applied Physics: Carbon Nanotubes: Synthesis, Structure, Properties, and Applications, Vol.80, Springer, Berlin, 2001.
[9] Bower C. A., Gilchrist K. H., Piascik J. R., Stoner B. R., Natarajan S., Parker C. B., Wolter S. D., Glass J. T., On-chip electro-impact ion source using carbon nanotube field emitters,

Appl. Phys. Lett. 90 (2007) 124102.

[10] YC Yang, L Qian, J Tang, L Liu, SS Fan, A low-vacuum ionization gauge with HfC-modified carbon nanotube field emitters, Appl. Phys. Lett. 92 (2008) 153105.

[11] Choi I. -M., Woo S. –Y., Song H. –W., Improved metrological characteristics of carbon-nanotube-based ionization gauge, Appl. Phys. Lett. 90 (2007) 023107.

[12] Kawano T., Chiamori H. C., Suter M., Zhou Q., Sosnowchik B. D., Lin L. W., An electrothermal carbon nanotube gas sensor, NanoLett. 7 (2007) 3686.

[13] Kaul A. B., Gas sensing with long, diffusively contacted single-walled carbon nanotubes, Nanotechnology 20 (2009) 155501.

[14] Choi J. W., Kim J. B., Batch-processed carbon nanotube wall as pressure and glow sensor, Nanotechnology 21 (2010) 105502.

[15] Han I. T., Kim H. J., Park Y. J., Lee N., Jang J. E., Kim J. W., Jung J. E., Kim J. M., Fabrication and characterization of gated field emitter arrays with self-aligned carbon nanotubes grown by chemical vapor deposition, Appl. Phys. Lett. 81 (2002) 2070.

[16] Lee Y. D., Lee K.S., Lee Y. H., Ju B. K., Field emission properties of carbon nanotube film using a spray method, Appl. Surf. Sci. 254 (2007) 513-516.

[17] Eklund P. C., Holden J. M., Jishi R. A., Vibrational modes of carbon nanotubes; spectroscopy and theory, Carbon 33 (1995) 959-972.

[18] Dresselhaus M. S., Eklund P. C., Phonons in carbon nanotubes, Adv. Phys. 49 (2000) 705-814.

[19] Zahab A., Spina L., Poncharal P., Marliere C., Water-vapor effect on the electrical conductivity of a single-walled carbon nanotube mat, Phys. Rev. B 62 (2000) 10000.

[20] Pati R., Zhang Y. M., Nayak S. K., Ajayan P. M., Effect of H_2O adsorption on electron transport in a carbon nanotube, Appl. Phys. Lett. 81 (2002) 2638.

[21] Neugebauer C. A., Webb M. B., Electrical conduction mechanism in unltrathin evaporated metal films, J. Appl. Phys. 33 (1962) 74-

[22] Rao C. N. R., Govindaraj A., Satishkumar B. C., Functionalised carbon nanotubes from solutions, Chem. Commun, 13 (1996) 1525-1526.

[23] Chen J., Hamon M. A., Hu H., Chen Y. S., Rao A. M., Eklund P. C., Haddon R. C., Solution properties of single-walled carbon nanotubes, Science 282 (1998) 95–98.

Authors: *Correspondence should be addressed to Dr. D. Z. Guo, Key Laboratory for Physics and Chemistry of Nanodevices, Department of Electronics, Peking University, Beijing 100871, China, E-Mail: guodz@pku.edu.cn; Miss J. Su, Email: sjbounce@163.com; Dr. Y. J. Xing, Email: xingyj@pku.edu.cn; Prof. G. M. Zhang, Email: zgmin@pku.edu.cn.*